AIAA JOURNAL
Vol. 35, No. 1, January 1997

Structural Damage Identification Using Assigned Partial Eigenstructure

Richard G. Cobb* and Brad S. Liebst†
U.S. Air Force Institute of Technology, Wright–Patterson Air Force Base, Ohio 45433-7765

A method of identifying damaged structural elements from measured modal data using an incomplete measurement set is presented. The method uses a mathematical optimization strategy to minimize deviations between measured and analytical modal frequencies and partial mode shapes. Damage is identified by determining the stiffness change to a finite element model required to match the measured data of the damaged structure. Damaged elements are obtained directly from the results of the cost-function minimization because the allowed structural changes are consistent with the original finite element formulation. The cost-function minimization is based on an assigned partial eigenstructure algorithm in which the physical properties of the structural elements are treated as control variables, which are chosen to achieve the measured partial eigenstructure. An iterative solution is used to solve the nonlinear optimization problem. Experimental results are reported for a cantilevered eight-bay truss assembly consisting of 104 elements.

Introduction

FUTURE large flexible space structures will have an unprecedented requirement of verifying on-orbit structural integrity on a periodic basis over the lifetime of the space system. Damage is possible during orbital maneuvers, docking operations, as well as collisions with space debris. Information on both location and extent of structural damage will be critical in assessing required in-space repair missions and/or deviations from the planned mission profiles.

To date, many methods have been proposed to compute structural damage from measured response data. These methods are based on either sensitivity analyses, residual nodal forces, assigned eigenstructures, or realization theories. Zimmerman and Smith[1] present a survey of the different techniques. A common requirement of these methods is the necessity to measure complete modal data, which is impractical and often impossible for large flexible structures. When only incomplete modal data are available, the common practice is to expand the measured data to the proper size using an eigenvector expansion method. A survey of mode-shape expansion techniques is presented by Hemez and Farhat.[2] Unfortunately, eigenvector expansion methods rely on the accuracy of the finite element (FE) model, which is the unknown when determining structural damage. Thus an alternative method that does not require full eigendata is desirable.

Presented is an algorithm to identify individual damaged structural elements of large flexible space structures using on-orbit measured data. Identification of modal frequencies, damping ratios, and shapes from on-orbit testing has been addressed by Kim and Bartkowicz.[3] Using measured partial eigendata, a control theoretic approach is applied in which fictitious actuators corresponding to each structural element are assumed. Using the measured partial eigendata and these fictitious actuators, an assigned partial eigenstructure (APE) technique is employed on the analytical model of the undamaged structure. An identification of structural damage is obtained directly from the control required of each fictitious actuator (stiffness adjustment) to achieve the measured eigenstructure.

The structural damage identification process can be divided into four main tasks: 1) identification of partial modal properties from measured data of the nominal space structure, 2) adjustment of the FE model to match the measured nominal partial data, 3) analysis of the extent to which structural damage can be localized to individual structural elements using the measured data, and 4) identification of structural damage using measured partial modal data from a damaged space structure. Previous work by the authors addressing the first three tasks is presented elsewhere.[4–6] Task 4 is the focus of the work contained herein.

Received May 11, 1996; revision received Aug. 24, 1996; accepted for publication Aug. 26, 1996; also published in *AIAA Journal on Disc*, Volume 2, Number 1. This paper is declared a work of the U.S. Government and is not subject to copyright protection in the United States.

*Captain, U.S. Air Force; currently Captain, U.S. Air Force, U.S. Air Force Phillips Laboratory, PL/VTSS, Kirtland Air Force Base, NM 87117-5776. Member AIAA.

†Associate Professor, Department of Aeronautics and Astronautics. Senior Member AIAA.

Theory

With minimal sensor information available, i.e., not every degree of freedom can be instrumented, a natural cost function representing the mismatch between the eigenstructure of the FE model and the measured partial eigendata is

$$J = \sum_{i}^{r} a_i \left(\frac{\lambda_i}{\bar{\lambda}_i} - 1 \right)^2 + \sum_{i}^{r} \sum_{j}^{s} b_{ij} (\phi_{ij} - \bar{\phi}_{ij})^2 \qquad (1)$$

The analytical eigenvalue for the ith mode is denoted as λ_i, and ϕ_{ij} denotes the jth element of the ith eigenvector from the analytical modal matrix $\mathbf{\Phi}$. The overbar indicates a measured quantity. The positive coefficients a_i and b_{ij} allow for individual weightings in the objective function. The summation upper limits r and s represent the number of eigenvalues/eigenvectors, and elements of the eigenvectors, respectively, from the measured data. A minimization of Eq. (1) was presented previously by the authors[5] to perform model updating using the software package ASTROS-ID, in which the minimization is solved using the eigenvalue and eigenvector sensitivities at each iteration step. Although this same technique can be used directly to identify structural damage, an alternative formulation that does not require the computation of the sensitivities and the corresponding eigenanalysis is accomplished using APE.

Structural damage identification using the APE method is based on minimizing the cost function given in Eq. (1). Two initial assumptions are made. First, structural damage is confined only to decreases in the stiffness properties of the structure. Second, structural damping is negligible. These two assumptions are consistent with most on-orbit damage scenarios of large flexible space structures. The free vibration of the undamaged structure is modeled as

$$M\ddot{\mathbf{x}} + K\mathbf{x} = 0 \qquad (2)$$

with the symmetric mass and stiffness matrices M, $K \in \Re^{n \times n}$, and $\ddot{\mathbf{x}}$ denoting a double time differentiation on the state vector $\mathbf{x}$. With damage confined to the stiffness matrix, the damaged structure is modeled as

$$M\ddot{\mathbf{x}} + (K - \Delta K)\mathbf{x} = 0 \qquad (3)$$

where ΔK represents an unknown perturbation to the stiffness as the result of structural damage. The eigenvalue and eigenvector for

the ith mode of Eq. (3) is given as (λ_i, Φ_i), whereas the measured eigenvalue and partial eigenvector for the same mode is represented as $(\bar{\lambda}_i, \bar{\phi}_i)$. The relationship between the n-dimensional eigenvector Φ_i and the partial eigenvector ϕ_i is $\phi_i = C\Phi_i$. The matrix $C \in \mathbb{R}^{s \times n}$ maps the full-length eigenvectors into the partial eigenvectors corresponding to the measured degrees of freedom.

For the APE method, the cost function in Eq. (1) is rewritten in vector notation and is given as

$$J = \frac{1}{2}(\lambda - \bar{\lambda})^T A(\lambda - \bar{\lambda}) + \frac{1}{2}\sum_{i=1}^{r}(\phi_i - \bar{\phi}_i)^T W_i(\phi_i - \bar{\phi}_i) \quad (4)$$

where $\lambda = [\lambda_1, \lambda_2, \ldots, \lambda_r]$ for the r measured modes. The positive-definite constant matrices A and W can be used to weight the contribution of each term in the overall cost function. This cost function then is minimized subject to the eigenstructure constraint

$$(-\lambda_i M + K - \Delta K)\Phi_i = 0 \quad (5)$$

where only r of the (λ_i, Φ_i) and only s components of Φ_i are measured. Additionally, to ensure that ΔK is consistent with the FE formulation, the structural constraint is represented as

$$\Delta K = BGB^T \quad (6)$$

where B is constructed from the nodal connectivity information and the elemental parameters and G is a diagonal matrix composed of the fraction of damage for each element.

This parameterization of ΔK is best illustrated using a simple example. For a two-degree-of-freedom spring-mass system as shown in Fig. 1, the equations of motion obtained from an application of Newton's second law and written in matrix form are

$$\begin{bmatrix} m_1 & 0 \\ 0 & m_2 \end{bmatrix}\ddot{\boldsymbol{x}} + \begin{bmatrix} k_1 + k_2 & -k_2 \\ -k_2 & k_2 \end{bmatrix}\boldsymbol{x} = 0 \quad (7)$$

The stiffness matrix K then can be written as

$$K = \begin{bmatrix} k_1 + k_2 & -k_2 \\ -k_2 & k_2 \end{bmatrix} = \begin{bmatrix} 1 & -1 \\ 0 & 1 \end{bmatrix}\begin{bmatrix} k_1 & 0 \\ 0 & k_2 \end{bmatrix}\begin{bmatrix} 1 & -1 \\ 0 & 1 \end{bmatrix}^T \quad (8)$$

The matrix premultiplying the diagonal matrix in Eq. (8) contains the structural connectivity information. For example, the first column of this matrix corresponds to spring k_1, which is connected only to degree-of-freedom x_1 and hence has only a single nonzero entry in row 1. The second column corresponds to spring k_2, which is connected to both degree-of-freedom x_1 and x_2, and hence both rows have nonzero entries. Direction cosines are used to determine the values of the nonzero entries, based on the relative position of the nodes. For this linear example, the direction cosines are $+1$ and -1. In the same fashion, the stiffness perturbation matrix ΔK can be expressed as

$$\Delta K = \begin{bmatrix} \sqrt{k_1} & -\sqrt{k_2} \\ \sqrt{k_1} & \sqrt{k_2} \end{bmatrix}\begin{bmatrix} g_1 & 0 \\ 0 & g_2 \end{bmatrix}\begin{bmatrix} \sqrt{k_1} & -\sqrt{k_2} \\ \sqrt{k_1} & \sqrt{k_2} \end{bmatrix}^T = BGB^T \quad (9)$$

Note that with $0 \le g_i \le 1$, any combination of decreases in the spring elements can be modeled in ΔK. In a similar fashion for a truss structure constructed from p rod elements, B and G are written as

$$B = [B_1 \quad \ldots \quad B_p] \quad (10)$$

$$B_i = \sqrt{(A_i E_i / L_i)} \times [0, \ldots, 0, c_1, c_2, c_3, 0, \ldots, 0, -c_1, -c_2, -c_3, 0, \ldots, 0]^T \quad (11)$$

$$G = \mathrm{diag}(g_1 \quad \ldots \quad g_p); \qquad 0 \le g_i \le 1 \quad (12)$$

with c_1, c_2, c_3 representing the direction cosines for the ith element, inserted at the degrees of freedom associated with the ith element. The variables A_i, E_i, and L_i are the cross-sectional area, elastic modulus, and length of the ith element, respectively. A damage fraction value of $g_i = 0$ corresponds to an undamaged element, whereas $g_i = 1$ corresponds to a complete loss of stiffness to the ith element. For beam elements with six degrees of freedom per node, the expression for B_i becomes

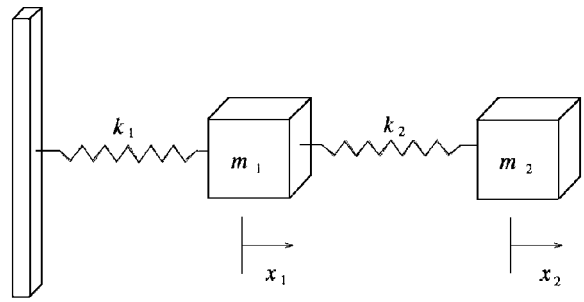

Fig. 1 Example of two-degree-of-freedom system.

$$B_i = R_i \cdot \begin{bmatrix} 1 & & & & & & & & & & & \\ & 2/L_i & & & & & & & & & & \\ & & 2/L_i & & & & & & & & & \\ & & & & & 1 & & & & & & \\ & & & -1 & & & & 1 & & & & \\ & & & & & & & & & 1 & & \\ -1 & & & & & & & & & & & \\ & -2/L_i & & & & & & & & & & \\ & & -2/L_i & & & & & & & & & \\ & & & & & -1 & & & & & & \\ & & & -1 & & & & -1 & & & & \\ & & & & & & & & & & -1 & \end{bmatrix} \times \mathrm{diag}\left[\frac{E_i}{L_i}(A_i \quad 3I_{1i} \quad 3I_{2i} \quad \mu_i j_i \quad I_{1i} \quad I_{2i})\right]^{\frac{1}{2}} \quad (13)$$

where R_i is the rotation matrix between the ith element's local coordinate frame, in which the inertia properties I_1 and I_2 are defined, and the global coordinate system. The variables μ_i and j_i are Poisson's ratio and the torsional stiffness of the ith element, respectively. Only the nonzero portion of B_i is shown, which occurs in the rows corresponding to the global degrees of freedom associated with the ith element. For beam elements, G is now a block diagonal matrix, with each diagonal block linked to a single design variable g_i ($g_i I_6$, where I_6 is the 6×6 identity matrix). The authors suspect that, although developed explicitly herein only for spring, rod, and beam elements, any element's symmetric matrix ΔK_i can be written as BG_iB^T using the nonzero singular values and singular vectors of ΔK_i, while preserving nodal connectivity.

The minimization of the cost function in Eq. (4) is solved by forming the Lagrangian and establishing and solving the necessary conditions. The appended cost function $\hat{J}_i$ for the ith mode is

$$\hat{J}_i = \tfrac{1}{2}a_i(\lambda_i - \bar{\lambda}_i)^2 + \tfrac{1}{2}(\phi_i - \bar{\phi}_i)^T W_i(\phi_i - \bar{\phi}_i) + \nu_i^T(-\lambda_i M + K - BGB^T)\Phi_i \quad (14)$$

where ν_i is a vector of Lagrange multipliers for the ith mode. With $\phi_i = C\Phi_i$, this becomes

$$\hat{J}_i = \tfrac{1}{2}a_i(\lambda_i - \bar{\lambda}_i)^2 + \tfrac{1}{2}(\Phi_i - \bar{\Phi}_i)^T C^T W_i C(\Phi_i - \bar{\Phi}_i) + \nu_i^T(-\lambda_i M + K - BGB^T)\Phi_i \quad (15)$$

It then is assumed that $\exists G \ni \lambda_i = \bar{\lambda}_i$, $\forall i = 1, \ldots, r$, implying that there are sufficient design variables (structural elements) to achieve the measured eigenvalues. This is satisfied if the measured data are consistent with actual damage. For the case of noise-corrupted measurements, $\lambda_i \approx \bar{\lambda}_i$, $\forall i = 1, \ldots, r$, and is assumed to contribute negligibly to the cost function. With these assumptions, Eq. (15) reduces to

$$\hat{J}_i = \tfrac{1}{2}(\Phi_i - \bar{\Phi}_i)^T C^T W_i C(\Phi_i - \bar{\Phi}_i) + \nu_i^T(-\bar{\lambda}_i M + K - BGB^T)\Phi_i \quad (16)$$

The necessary conditions for the minimization become

$$\frac{\partial \hat{J}_i}{\partial \nu_i} = (-\bar{\lambda}_i M + K - BGB^T)\Phi_i = 0 \tag{17}$$

$$\frac{\partial \hat{J}_i}{\partial G} = \frac{\partial}{\partial G}(\nu_i^T BGB^T \Phi_i) = 0 \tag{18}$$

$$\frac{\partial \hat{J}_i}{\partial \Phi_i} = C^T W_i C(\Phi_i - \bar{\Phi}_i) + [\nu_i^T(-\bar{\lambda}_i M + K - BGB^T)]^T = 0 \tag{19}$$

which can be rewritten as

$$(-\bar{\lambda}_i M + K)\Phi_i - BGB^T \Phi_i = 0 \tag{20}$$

$$\frac{\partial}{\partial G}(\nu_i^T BGB^T \Phi_i) = 0 \tag{21}$$

$$C^T W_i C\Phi_i + (-\bar{\lambda}_i M + K)\nu_i - BGB^T \nu_i = C^T W_i \bar{\phi}_i \tag{22}$$

To pose this nonlinear optimization problem as an approximate linear problem, it is necessary to introduce the matrix operator $\tilde{P}(\alpha, \beta)$. In the case where there is only one column of the matrix B associated with each design variable, such as for spring and rod elements as given in Eqs. (9–12), $\tilde{P}(\alpha, \beta)$ is defined as

$$\tilde{P}(\alpha, \beta) \quad \text{with} \quad \tilde{P} \quad \text{and} \quad \beta \in \Re^{n \times p}, \qquad \alpha \in \Re^{n \times 1}$$
$$\tilde{P}_{ij} = \sum_{k=1}^{n} \alpha_k \beta_{ij} \beta_{kj} \tag{23}$$

where $\tilde{P}_{ij}$ is the ith row and the jth column of the matrix $\tilde{P}$. In terms of the operator $\tilde{P}$, terms of the form $\beta\Gamma\beta^T\alpha$ can be written as

$$\beta\Gamma\beta^T\alpha = \tilde{P}(\alpha, \beta)\gamma \quad \text{where} \quad \gamma = \text{diag}(\Gamma)$$
$$\Gamma \in \Re^{p \times p}(\text{diag}) \tag{24}$$

When there are multiple columns of B associated with a single design variable, such as given in Eq. (13) for beam elements, an additional summation of the columns of $\tilde{P}$ is required for each design variable. In the case where there are q columns of B for each design variable, $B \in \Re^{n \times pq}$, $G \in \Re^{pq \times pq}$, and hence, $\tilde{P} \in \Re^{n \times pq}$ according to Eq. (23). The summation is then defined as

$$P = \left[\sum_{j=1}^{q} \tilde{P}_j \quad \sum_{j=q+1}^{2q} \tilde{P}_j \quad \cdots \quad \sum_{j=(p-1)q+1}^{pq} \tilde{P}_j \right], \quad P \in \Re^{n \times p} \tag{25}$$

where $\tilde{P}_j$ is the jth column of $\tilde{P}$. Note that $P = \tilde{P}$ for the case where $q = 1$. Furthermore, constructing P from $\tilde{P}$ gives the design engineer the ability to link multiple elements to a single design variable g_i as desired. For example, consider the system described by Fig. 1 and Eq. (9). If

$$\Phi_i = \begin{Bmatrix} \phi_1 \\ \phi_2 \end{Bmatrix} \tag{26}$$

then

$$P(\Phi_i, B) = \begin{bmatrix} k_1\phi_1 & k_2\phi_1 - k_2\phi_2 \\ 0 & -k_2\phi_1 + k_2\phi_2 \end{bmatrix} \tag{27}$$

In terms of the operator P and $\boldsymbol{g} = \text{diag}(G)$, the following substitutions can be made in the necessary conditions:

$$BGB^T\Phi_i = P(\Phi_i, B)\boldsymbol{g} \tag{28}$$

$$\frac{\partial}{\partial G}(\nu_i^T BGB^T \Phi_i) = P(\Phi_i, B)^T \nu_i \tag{29}$$

$$BGB^T\nu_i = P(\nu_i, B)\boldsymbol{g} \tag{30}$$

The necessary conditions, with these substitutions, become

$$(-\bar{\lambda}_i M + K)\Phi_i - P(\Phi_i, B)\boldsymbol{g} = 0 \tag{31}$$

$$P(\Phi_i, B)^T \nu_i = 0 \tag{32}$$

$$C^T W_i C\Phi_i + (-\bar{\lambda}_i M + K)\nu_i - P(\nu_i, B)\boldsymbol{g} = C^T W_i \bar{\phi}_i \tag{33}$$

which now can be written in matrix form for the ith mode as

$$\begin{bmatrix} (-\bar{\lambda}_i M + K) & 0 & -P(\Phi_i, B) \\ 0 & P(\Phi_i, B)^T & 0 \\ C^T W_i C & (-\bar{\lambda}_i M + K) & -P(\nu_i, B) \end{bmatrix} \begin{bmatrix} \Phi_i \\ \nu_i \\ \boldsymbol{g} \end{bmatrix} = \begin{bmatrix} 0 \\ 0 \\ C^T W_i \bar{\phi}_i \end{bmatrix} \tag{34}$$

Then, because $\boldsymbol{g}$, the vector of fractional structural damage for each element (g_i), must be the same for each measured mode, the necessary conditions can be assembled as

$$N \begin{bmatrix} \Phi_1 \\ \nu_1 \\ \vdots \\ \Phi_r \\ \nu_r \\ \boldsymbol{g} \end{bmatrix} = \begin{bmatrix} 0 \\ 0 \\ C^T W_1 \bar{\phi}_1 \\ \vdots \\ 0 \\ 0 \\ C^T W_r \bar{\phi}_r \end{bmatrix} \tag{35}$$

where

$$N = \begin{bmatrix} (-\bar{\lambda}_1 M + K) & & & -P(\Phi_1, B) \\ & P(\Phi_1, B)^T & & \\ C^T W_1 C & (-\bar{\lambda}_1 M + K) & & -P(\nu_1, B) \\ & & \ddots & \vdots \\ (-\bar{\lambda}_r M + K) & & & -P(\Phi_r, B) \\ & P(\Phi_r, B)^T & & \\ C^T W_r C & (-\bar{\lambda}_r M + K) & & -P(\nu_r, B) \end{bmatrix} \tag{36}$$

and $N \in \Re^{(2n+p)r \times (2nr+p)}$, representing an overdetermined set of equations whenever $r > 1$. Note that only the nonzero entries are shown. The desired solution vector $\boldsymbol{g}$ then is found from a least-squares solution to Eq. (35) using a QR decomposition and back substitution.[7] Because $N = N(\Phi_i, \nu_i)$, an iterative scheme is introduced updating (Φ_i, ν_i) with the results of the previous iteration. The initial guess at (Φ_i, ν_i) is to use the nominal vector Φ_i from the undamaged model, with the measured $\bar{\phi}_i$ elements inserted at the measured degrees of freedom. It is assumed that the structural damage was not catastrophic, and thus the nominal eigenvectors are a reasonable initial guess. Vector normalization and sign convention are accounted for by setting $\|C\Phi_i\|_2 = \|\bar{\phi}_i\|_2 = 1$ and $(C\Phi_i)^T \cdot \bar{\phi}_i > 0$. The Lagrange multiplier vector ν_i is initially assumed to be zero. During the iteration process, values of the damage

fraction g_i outside the allowable range $0 \leq g_i \leq 1$ are removed from subsequent iterations, further reducing the parameter search space. The weighting matrix W_i is nominally set to the identity matrix (scaled such that $\|W_i\| \approx \|K\|$) corresponding to the case where all measurements are assumed at the same level of uncertainty.

Software Implementation

Structural damage identification using APE proceeds as follows. First, the matrix B is constructed according to Eq. (11) for rod elements, or Eq. (13) for beam elements. A B_i is constructed for each element in the search space. Next, using the mass and stiffness matrices M and K from a tuned FE model (one in which the measured data of the undamaged structure correlate well with the model) and the measured eigendata of the damaged structure, Eq. (35) is constructed. A QR decomposition and backsubstitution is used to solve for the achievable eigenvectors Φ_i, the Lagrange multipliers ν_i, and the damage fractions g_i. Elements in $\boldsymbol{g}$ outside an allowable range (i.e., an increase in stiffness or negative stiffness) are removed from the search space by removing the corresponding columns of B. At each iteration step, the matrix N is updated using either the new (Φ_i, ν_i) solution pair or the new reduced B matrix. The solution sequence is repeated until convergence. The flowchart for this algorithm is shown in Fig. 2.

For the initial construction of N using the measured $(\bar{\lambda}_i, \bar{\phi}_i)$ data, two preprocessing steps are required. The first is a pairing of the measured mode shapes with the analytical nominal mode shapes. This is accomplished by normalizing the ∞ norm of the partial mode shapes to unity and then checking the cross-orthogonality relation as given in the following:

$$O = \phi^T \bar{\phi}, \qquad \phi \quad \text{and} \quad \bar{\phi} \in \Re^{s \times r} \tag{37}$$

Modes are paired on the basis of the row and column positions of the maximum values in the matrix O. A second check is performed to verify that the measured modal frequencies of the damaged structure are at or below the corresponding frequencies of the undamaged analytical model, i.e., $\bar{\lambda}_i \leq \lambda_i \ \forall i$. For each mode, measured frequencies above the analytical frequencies are set to the analytical values. This is done because structural damage, when confined to decreases in the stiffness matrix, can only decrease the natural frequencies. This requirement can be shown easily by establishing the negative definiteness of changes in the eigenvalues to changes in the stiffness matrix. Using the same approach as that developed by Fox and Kapoor,[8] these changes to first order can be expressed as

$$\frac{\partial \lambda}{\partial \boldsymbol{g}} = -\Phi^T P(\Phi, B) \tag{38}$$

For this first-order model, it is sufficient to show the negative definiteness of the ith eigenvalue with respect to the jth stiffness value change. This relationship is given as

$$\frac{\partial \lambda_i}{\partial g_j} = -\Phi_i^T P(\Phi_i, B_j) \tag{39}$$

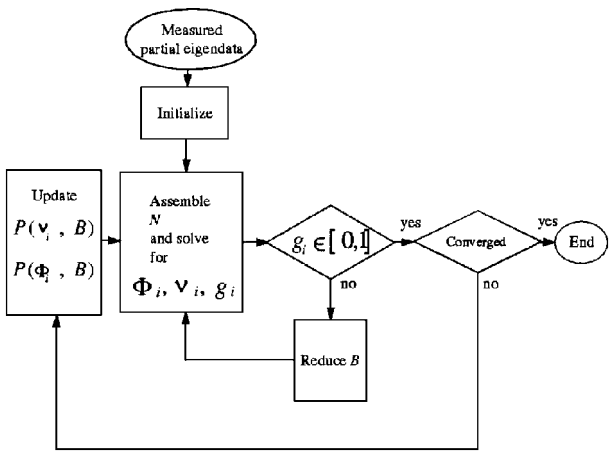

Fig. 2 APE decision flow.

By using the definition of P from Eq. (23), which is valid for rod elements, and carrying out the vector multiplication, Eq. (39) yields

$$\frac{\partial \lambda_i}{\partial g_j} = -\sum_{k=1}^{n}\sum_{l=1}^{n} \Phi_{li}\Phi_{ki} B_{lj} B_{kj} \tag{40}$$

Rearranging the summation yields

$$\frac{\partial \lambda_i}{\partial g_j} = -\sum_{k=1}^{n} \Phi_{li} B_{lj} \sum_{k=1}^{n} \Phi_{ki} B_{kj} \tag{41}$$

which simplifies to

$$\frac{\partial \lambda_i}{\partial g_j} = -\left(\sum_{l=1}^{n} \Phi_{li} B_{lj} \right)^2 \tag{42}$$

which is a negative-definite quantity. If the more general definition of P is used as given in Eq. (25), an additional summation is required over the corresponding columns of B associated with the jth design variable. Again, this is a negative-definite quantity because it is the sum of negative-definite terms from Eq. (42).

The APE iterative solution technique involves the least-squares solution of the matrix N in Eq. (36). This matrix is classified as a large sparse rectangular matrix that is possibly singular, and therefore the solution technique is tailored to this matrix classification. A sparse QR algorithm is used to decompose N and then a backsubstitution to compute the solution vector. Because of the size of N, a sparse solver is required for all but small pedagogical problems. Column pivoting in the QR decomposition is not incorporated because pivoting does not preserve the matrix sparsity and increases the number of fill-ins. For the case when N is singular, the nature of the solution is different than that of the Moore–Penrose pseudoinverse. The solution vector contains as many zero entries as the rank deficiency of N. This is a desirable attribute when used for damage identification because, typically, damage is localized in the structure, and hence only a small number of elements have nonzero damage fractions. The APE algorithm was coded using MATLAB® (Ref. 9), with portions written in Fortran to handle the sparse matrix manipulations to speed processing time. MATLAB's spqrmex algorithm was used to perform the decomposition. In practice, the range of allowable damage fractions ($0 \leq g_i \leq 1$) was widened to ensure that g_i were not discarded prematurely before convergence.

An additional consideration in damage identification algorithms is that of uniqueness. With only partial modal data available, the problem is generally ill-posed and hence there may exist multiple damage fractions that result in the same partial eigendata. This problem is exacerbated when noise-corrupted measurements are used. The use of the structural constraint as given in Eq. (6), combined with the restriction that the damage fraction g_i lies within an allowable range, helps to minimize the problem of nonuniqueness. For a given problem, solution uniqueness is dependent on the number of modes, the number of eigenvector components measured, the quality (signal/noise) of the measurements, the FE model, and the numerical accuracies of the identification algorithm. To account for nonunique solutions in the APE method, an off-line sensitivity analysis can be performed once the size and quality of the measurement set has been determined. Using the results of this analysis, the parameter search space can be confined to elements that produce unique and identifiable eigenstructures. Elements whose damage results in an identifiable change in the measured partial eigenstructure [J value in Eq. (1)] are defined as detectable. Next, APE symmetric elements are defined as a group of damaged structural elements that produce the same measured partial eigenstructure. With these definitions, the results of the APE method indicate damage fractions that are confined to an APE symmetric element set. Further refinement to an individual element within the set is not possible without additional or higher-quality measurement data. Further discussions on the topic of nonunique solutions, including a method to perform the sensitivity analysis, are presented elsewhere.[6]

Numerous tests of the APE method were conducted using FE models of sizes ranging between 16 and 192 degrees of freedom constructed of 8 to 104 structural elements using either spring, rod,

or beam elements. In all cases, when using analytical eigendata simulating both perfect measurements and perfect model correlation, the APE method converged to the correct damaged element(s), and indicated the correct percent of damage. In each case, less than 10% of the total degrees of freedom was included in the measurement set, and only a small number of the natural frequencies. An additional attribute of the algorithm is that, in the case where the entire eigenvector can be measured perfectly, the exact solution is obtained without iterating.

Experimental Demonstration

An experimental validation of the APE method was conducted using NASA test data of an experimental truss. NASA's eight-bay truss test bed consisted of eight cubic bays of a hybrid space truss cantilevered from a rigid backstop plate (see Fig. 3). This configuration represents a scaled section of the proposed International Space Station. Each bay is a half-meter in length and constructed of aluminum members. The truss contains three types of elements: battens (elements parallel to either the x or the z axis), longerons (elements parallel to the y axis), and diagonals (elements not parallel to any of the axes). The truss was fully instrumented with one triaxial accelerometer at each of its 32 unconstrained nodes. Disturbance excitation was achieved using two ground-based dynamic shakers attached at two different node points. Figure 4 shows a typical measured frequency response function for both the nominal and the damaged structures. From these frequency responses the first five system natural frequencies could be determined. A complete description of the hardware and the testing procedure is contained in the work of Kashangaki.[10]

For use of the test data herein, two different test configurations were assumed. The first was that all of the data from each of the 96 unconstrained degrees of freedom were available for use in the damage identification algorithm. This is referred to as the fully instrumented configuration. Second, the data set was arbitrarily limited to the use of data from only eight unconstrained degrees of freedom. This is referred to as the sparsely instrumented configuration.

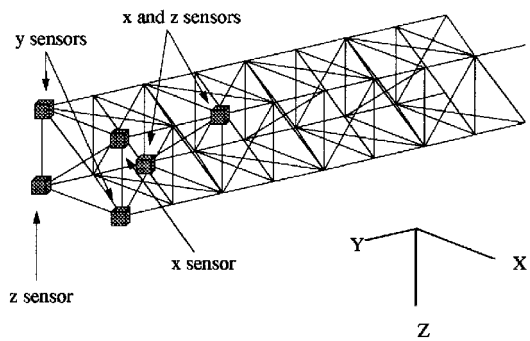

Fig. 3 Prioritized sensor locations for the NASA truss.

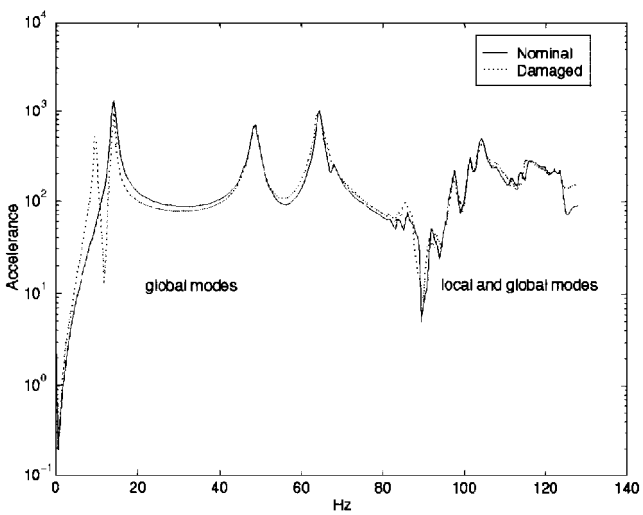

Fig. 4 Measured frequency response functions for the NASA truss.

Table 1 Measured natural frequencies of NASA's eight-bay truss

	Frequency, Hz			% Difference	
Mode no.	Measured	Initial	Tuned	Initial	Tuned
1	13.88	13.79	13.88	0.65	0.00
2	14.48	14.31	14.47	1.19	0.07
3	48.41	50.53	48.40	4.37	0.02
4	64.03	65.98	64.03	3.05	0.00
5	67.46	71.20	67.52	5.55	0.08

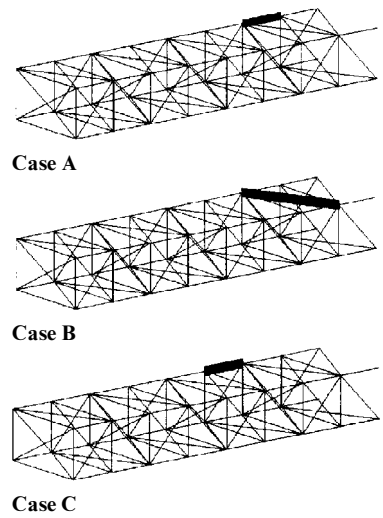

Fig. 5 Damage configurations for the NASA truss, cases A–C.

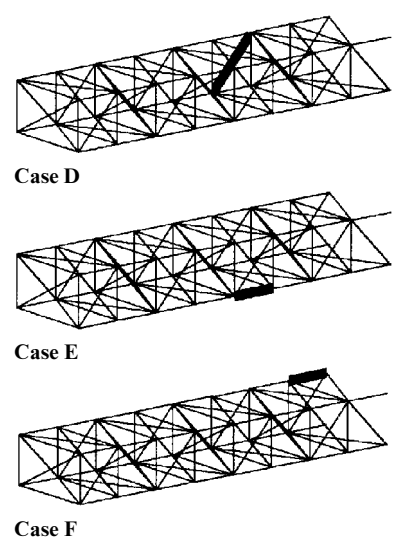

Fig. 6 Damage configurations for the NASA truss, cases D–F.

For each configuration, nine damage cases were tested. The damage cases were the full removal of one or two elements of the truss. The different damage cases are shown in Figs. 5–7. For the nominal case, i.e., no damage, the results of the FE analysis and the measured data are compared in Table 1. Although the FE model is in fair agreement with the measured data, any disagreement will result in the damage identification method assigning a percentage of damage to an element(s) to account for the disagreement. Therefore, tuning was performed using ASTROS-ID (Ref. 5) to ensure that the initial disagreement was as minimal as possible. The resulting frequencies after tuning are listed in Table 1.

Using the tuned model, an eigenanalysis for each of the nine damage cases was performed. The results, along with the experimentally measured data from the damaged structure, are presented in Table 2 for comparison. For the objective function minimization to be successful, it is important that the analytical model with simulated damage correlate well with the measured data of the damaged structure. As can be seen from the results in Table 2, the analytical model

Table 2 Changes in natural frequencies from damage on the NASA truss

Damage case	Frequency, Hz				
	Mode 1	Mode 2	Mode 3	Mode 4	Mode 5
Nominal	13.88/13.88[a]	14.48/14.47	48.41/48.40	64.03/64.03	67.46/67.52
A	13.94/13.88	9.50/9.43	48.52/48.40	64.16/64.03	65.91/64.98
B	13.47/13.16	14.12/14.25	35.65/34.25	60.18/59.06	65.86/65.90
C	13.97/13.88	11.39/11.29	48.53/48.40	64.50/64.03	59.90/58.51
D	13.21/13.16	14.44/14.24	36.68/35.92	61.35/61.20	66.95/65.97
E	13.96/13.88	11.42/11.30	48.57/48.40	64.61/64.03	59.91/58.60
F	13.94/13.88	9.50/9.42	48.50/48.40	64.08/64.03	65.80/64.91
G	12.29/12.26	14.50/14.47	48.67/48.40	50.65/48.60	67.76/67.52
H	13.73/13.70	14.55/14.47	48.68/48.40	54.76/54.30	67.71/67.52
I	13.74/13.58	9.86/9.74	36.66/35.89	63.35/62.56	58.86/57.46

[a]Data presented in (measured/FE simulated) format, where the first number represents the measured frequency and the second is the result of an eigenanalysis on the FE model with the damaged element(s) removed.

Table 3 APE identification results on the NASA truss, fully instrumented

Damage case	True damage		APE identified		
	Element no.	% Damage	Element no.	% Damage	CPU time, s
A	84	100	84	88	241
B	85	100	85	96	184
			43[a]	102	
C	71	100	71	95	302
D	78	100	78	98	262
			96	109	
E	62	100	62	95	288
			70	78	
			92	124	
F	97	100	97	89	194
G	51	100	51	96	460
H	34	100	34	98	367
			43[a]	108.2	
I	71	100	71	94	289
	78	100	78	99	

[a]Element attached to degree of freedom with faulty sensor.

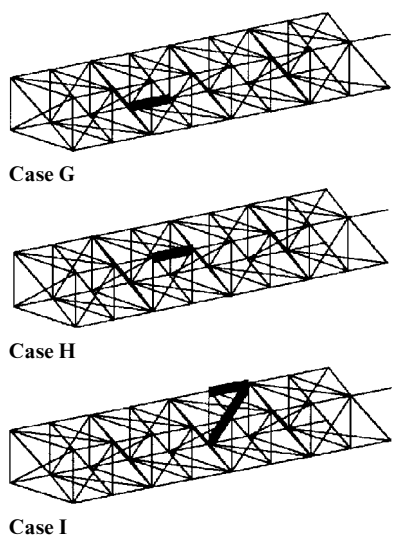

Case G

Case H

Case I

Fig. 7 Damage configurations for the NASA truss, cases G–I.

is in fair agreement for the nominal as well as the damage cases. The largest deviations between the measured and simulated damaged analytical model occurred for damage case I, the compound break.

Damage identification for the fully instrumented truss using APE was performed using a search space consisting of all 104 elements of the truss. The measured data consisted of the first five flexible modes and the entire measured eigenvector for each mode. The results are contained in Table 3. In all nine cases, the damaged element was correctly identified. For cases B and H, element 43 also was identified as damaged. Previous work by Zimmerman et al.[11] reported that there was a failed sensor at degree-of-freedom44. One end of element 43 is attached at degree-of-freedom44. For cases D and E, element 96 (case D) and elements 70 and 92 (case E) also were identified as damaged. These three elements are all batten elements that have negligible effect on the cost function when using only the first five modes. Also noted in some cases are assigned damage values that are greater than 100%. As previously discussed, to avoid prematurely discarding elements and to allow for modeling error, the allowable range of $\boldsymbol{g}$ should be widened. For the results reported, the allowable range was set to ($0 \leq g_i \leq 2$). Once again, an off-line sensitivity analysis of the g_i boundaries should be performed. The authors are currently working on software modifications to make the g_i boundary limits adaptive with increasing iterations.

Table 4 Damage localization results for the NASA eight-bay truss

Element no.	Equivalent symmetric elements
32	36, 45, 49
34	38
47	51, 60, 64
58	62, 71, 75
59	
61	
63	
65	
72	
73	77, 86, 90
74	
76	
78	
84	88, 97, 101
85	
87	
89	
91	
98	
99	103
100	
102	
104	
Undetectable elements	1–31, 33, 35, 37, 39–44, 46, 48, 50, 52–57, 66–70, 79–83, 92–96

A second test configuration was performed using measurement data from only eight sensor locations. After tuning the analytical model, a prioritization of which of the eight degrees of freedom to instrument was performed as developed elsewhere.[6] The eight prioritized sensor locations are shown in Fig. 3. These eight degree-of-freedom locations were used to construct the eight elements of the partial eigenvectors for the damage identification process.

After selecting the eight sensor locations, a damage localization analysis was performed as described elsewhere.[6] The results of this analysis are contained in Table 4, listing the undetectable, symmetric, and identifiable elements as previously defined. Table 5 presents a description of the element numbering used. The results show that, using only the first five modes and the five 8-component eigenvectors, 64 of the elements are undetectable from the measured data.

Table 5 Element numbering and descriptions for the NASA eight-bay truss

Bay no.[a]	Description		
	Longeron	Diagonal	Batten[b]
1	6, 8, 10, 12	7, 9, 11, 13	1, 2, 3, 4, 5
2	19, 21, 23, 25	20, 22, 24, 26	14, 15, 16, 17, 18
3	32, 34, 36, 38	33, 35, 37, 39	27, 28, 29, 30, 31
4	45, 47, 49, 51	46, 48, 50, 52	40, 41, 42, 43, 44
5	58, 60, 62, 64	59, 61, 63, 65	53, 54, 55, 56, 57
6	71, 73, 75, 77	72, 74, 76, 78	66, 67, 68, 69, 70
7	84, 86, 88, 90	85, 87, 89, 91	79, 80, 81, 82, 83
8	97, 99, 101, 103	98, 100, 102, 104	92, 93, 94, 95, 96

[a]Bays are numbered consecutively starting from the free end.
[b]Includes diagonal members in the batten plane.

Table 6 APE identification results on the NASA truss, sparsely instrumented

Damage case	True damage		APE identified		
	Element no.	% Damage	Element no.	% Damage	CPU time, s
A	84	100	84(88, 97, 101)[a]	85	33
B	85	100	85	96	80
C	71	100	58(62, 71, 75)	94	65
D	78	100	78	98	76
			104	110	
E	62	100	58(62, 71, 75)	110	56
			32(36, 45, 49)	103	
F	97	100	84(88, 97, 101)	89	32
G	51	100	47(51, 60, 64)	88	85
H	34	100	34(38)	97	43
I	71	100	32(36, 45, 49)	80	63
	78	100	78	99	

[a]Data presented in I(S) format, where I is the number of the identified element and S is the symmetric element numbers.

This indicates that changes in the measured data are insignificant from damage in these elements. These results are consistent with a similar analysis on this truss presented by Kashangaki et al.[12] showing that 95% of the total strain energy associated with the first six modes was contained in only 40 elements. The unidentifiable elements are categorized as either battens, or elements located near the free end of the truss. The remaining 40 elements of the localization analysis are divided among 23 symmetric groupings containing one, two, or four elements. One element from each of the 23 symmetric groups is used to define the initial search space for the identification process.

Using the results of the sensor prioritization to define the measured data, the tuned analytical model, and the damage localization analysis to define the initial search space, damage identification using APE was performed. The results are contained in Table 6. On average, the results were achieved in 1 min of CPU time on a Sparc-10 workstation and required 20 iterations. In six of the nine cases, the damage was localized to a single element or a single symmetric grouping. For cases D and E, a repeated use of the APE method, using the results of the first identification application as the initial search space, was able to localize the damage down to the single correct element or single symmetric group. A capability could be incorporated into the APE algorithm to adaptively reinitialize the algorithm. For damage case I—the compound break—damage to element 71 was not identified. Damage to element 71 (a longeron in the sixth bay) was assigned to a longeron in either bay 3 or 4. This difficulty is, in part, due to the fact that the measured data for this damage case do not correlate well with the simulated damaged analytical model, as indicated by the values given in Table 2. The true culprit, modeling error or measurement error, cannot be determined from the known information. Anytime the simulated damage to the analytical model does not agree with the measured data for the same damage configuration, any method based on matching the partial measured data will have difficulty in obtaining the true solution.

Conclusions

A method was presented to identify damaged structural elements from limited measurement data. Damage identification was performed using a newly developed APE method, which determines the required stiffness changes consistent with the FE formulation, to achieve the measured eigendata. This method does not require the computation of the eigenstructure sensitivities and the corresponding eigenanalysis during the iteration process. It does, however, require the decomposition of a large sparse matrix requiring sparse matrix techniques to make it computationally competitive. This method was demonstrated on both a fully instrumented and a sparsely instrumented experimental structure, correctly determining the location and amount of structural damage. The extent to which damage can be localized was limited by both model fidelity and accuracy of the measured modes.

Acknowledgment

Special thanks to T. Kashangaki who provided the experimental data on the NASA truss.

References

[1]Zimmerman, D. C., and Smith, S. W., "Model Refinement and Damage Detection for Intelligent Structures," *Intelligent Structural Systems*, edited by H. S. Tzou, Kluwer Academic, Norwell, MA, 1992, pp. 403–452.

[2]Hemez, F., and Farhat, C., "Comparing Mode Shape Expansion Methods for Test-Analysis Correlation," *Proceedings of the 12th International Modal Analysis Conference* (Honolulu, HI), Society for Experimental Mechanics, Bethel, CT, 1994, pp. 1560–1567.

[3]Kim, H. M., and Bartkowicz, T. J., "Damage Detection and Health Monitoring of Large Space Structures," *Journal of Sound and Vibration*, Vol. 27, June 1993, pp. 12–17.

[4]Cobb, R. G., and Liebst, B. S., "Structural Damage Identification from Frequency Response Data," *Proceedings of the 1995 Guidance, Navigation and Control Conference* (Baltimore, MD), AIAA, Washington, DC, 1995, pp. 334–344.

[5]Cobb, R. G., Canfield, R. A., and Liebst, B. S., "Finite Element Model Tuning Using Automated Structural Optimization System Software," *AIAA Journal*, Vol. 34, No. 2, 1996, pp. 392–399.

[6]Cobb, R. G., and Liebst, B. S., "Sensor Location Prioritization and Structural Damage Localization Using Minimal Sensor Information," *Proceedings of the International Conference on Identification in Engineering Systems* (Swansea, Wales, UK), Univ. of Wales, Swansea, Wales, UK, 1996, pp. 275–284.

[7]Golub, G. H., and Van Loan, C. F., *Matrix Computations*, 1st ed., Johns Hopkins Univ. Press, Baltimore, MD, 1983, Chap. 7.

[8]Fox, R. L., and Kapoor, M. P., "Rates of Change of Eigenvalues and Eigenvectors," *AIAA Journal*, Vol. 6, No. 12, 1968, pp. 2426–2429.

[9]Anon., "MATLAB®: High Performance Numeric Computation and Visualization Software," Math Works, Natick, MA, 1994.

[10]Kashangaki, T. A. L., "Ground Vibration Tests of a High Fidelity Truss for Verification of on Orbit Damage Location Techniques," NASA-TM-107626, May 1992.

[11]Zimmerman, D. C., Simmermacher, T., and Kaouk, M., "Model Correlation and System Health Monitoring Using Frequency Domain Measurements," *Proceedings of the 36th Structures, Structural Dynamics, and Materials Conference* (New Orleans, LA), AIAA, Washington, DC, 1995, pp. 3318–3326.

[12]Kashangaki, T. A. L., et al., "Underlying Modal Data Issues for Detecting Damage in Truss Structures," *Proceedings of the 33rd Structures, Structural Dynamics, and Materials Conference* (Dallas, TX), AIAA, Washington, DC, 1992, pp. 1437–1446.